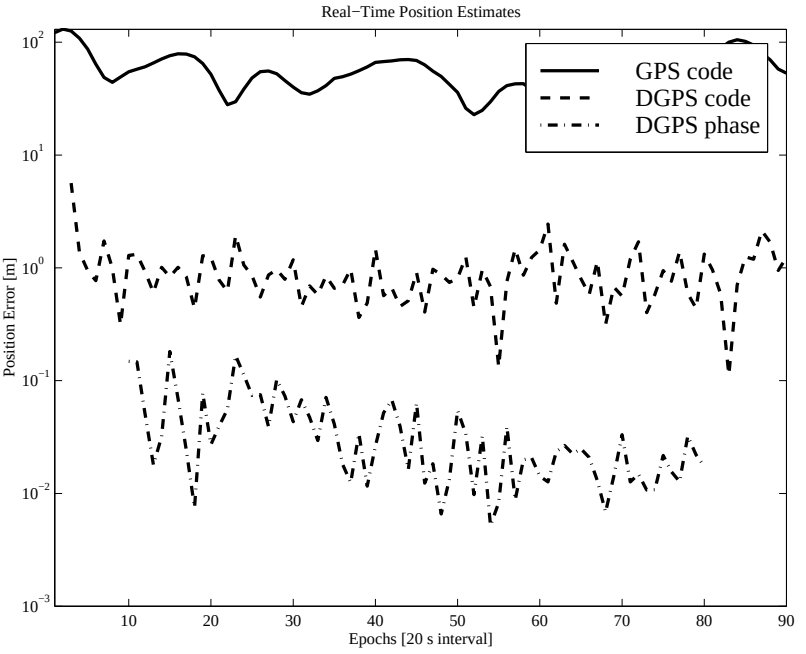

Figure 20.1 Real-time position accuracy

Real-Time Positioning Accuracy

Accuracy of GPS-based position estimates obtained in real time can range from tens of meters to centimeters depending upon the user's resources. In the following we rely on ideas from Misra & Burke & Pratt (1999).

Figure 20.1 illustrates three levels of positioning accuracy obtained from GPS in real time with position errors ranging from tens of meters to centimeters. The 3-D position error is plotted for observations taken at 20-s intervals over a period of half an hour. Figure 20.1 is created by the *M*-file rtk5.

The raw L_1 code position accuracy has typical error of tens of meters. Access to concurrent observations from a GPS receiver at a known location in the area reduces the errors in the position estimates to meter level and decimeter level depending upon the data transferred on a radio link from the reference station to the user.

Finally the full potential of the observations is exploited to obtain centimeter-level position estimates.

Error Analysis of One-Ways

Our objective is to offer a qualitative appreciation for the nature and magnitude of the errors. The errors show considerable variability. We follow ideas presented in Misra & Burke & Pratt (1999).

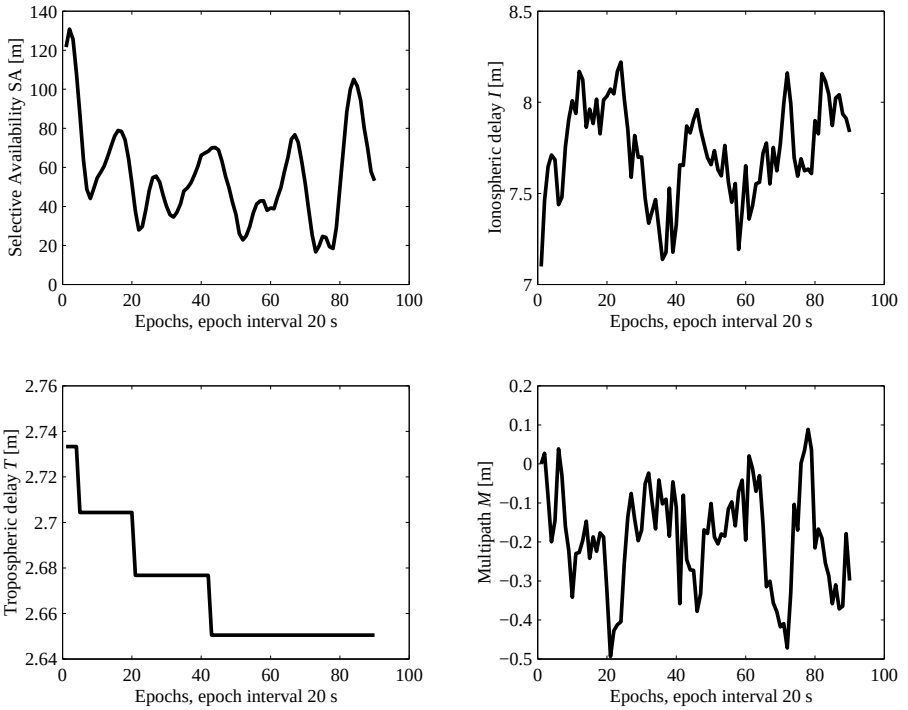

Figure 20.2 One-way errors

We consider a one-way observed at a station south of Aalborg from day 76 of 1994. We only consider L_1 code for PRN 02 in the time interval from 9:42 a.m. to 10:11 a.m. local time. The satellite elevation angle is circa 60°. In estimation of these errors we have taken advantage of information generally not available for a user: we know our position precisely. In four subplots we demonstrate the error from SA, ionosphere, troposphere, and multipath. Figure 20.2 is created by oneway_e. The four subplots are available as individual plots under the names err1.eps, err2.eps, err3.eps, and err4.eps.

SA error can be modelled as a Gauss-Markov process with zero-mean, standard deviation of about 24 m, and correlation time of 3–4 minutes.

When dealing with the ionospheric delay we assume that we have both code and phase observations on L_1 and L_2 at our disposal. We estimate the delay I according to the matrix equation on page 507:

$$\begin{bmatrix} 1 & 1 & 0 & 0 \\ 1 & -1 & \lambda_1 & 0 \\ 1 & \beta & 0 & 0 \\ 1 & \beta & 0 & \lambda_2 \end{bmatrix} \begin{bmatrix} \rho^* \\ I \\ N_1 \\ N_2 \end{bmatrix} = \begin{bmatrix} P_1 \\ \Phi_1 \\ P_2 \\ \Phi_2 \end{bmatrix} - \boldsymbol{e}. \tag{20.1}$$

First we estimate N_1 and N_2 and next we estimate ρ^* and I alone.

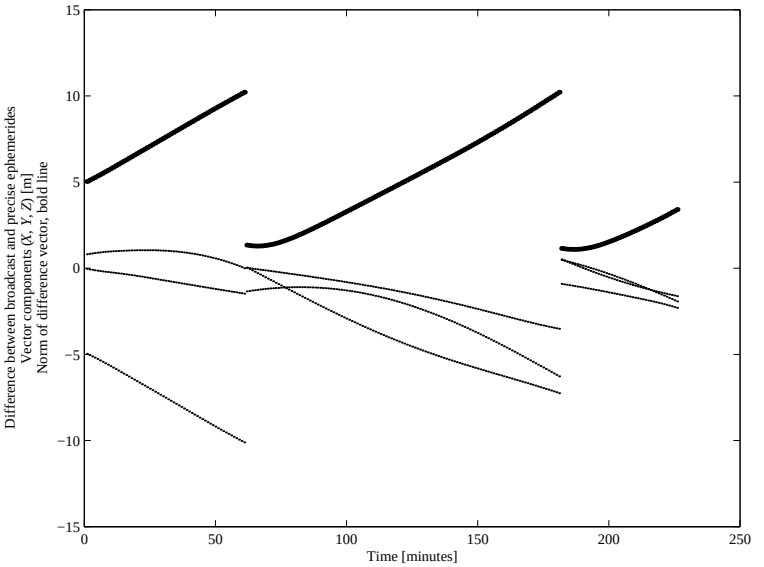

Figure 20.3 Difference between precise and broadcast ephemerides

For the tropospheric delay we use the Goad-Goodman model. The delay T ranges from 2.74 m to 2.65 m. If the satellite had come directly overhead, the corresponding delay would have been about 2.5 m.

Remaining errors are identified as multipath and receiver noise. The error is below 1 m except for low satellite elevation angles and shows sinusoidal oscillations with a period of 5–10 min characteristic of multipath.

Finally we investigate the difference between precise and broadcast ephemerides. Figure 20.3 shows the difference in satellite position as computed from broadcast ephemerides given via the navigation file, and the post-processed satellite positions. These positions are downloaded in SP3 format from `igscb.jpl.nasa.gov/components/prods_cd.html`. The SP3 format contains for every 15 minutes the (X, Y, Z) position of each satellite. A Lagrange interpolation of at least 7th order is used to compute the actual position.

The ephemeris error vector also was projected onto the line of sight, see Figure 20.4. The discontinuities in the error reflect the routine ephemeris updates at 2-h intervals. The observed ephemeris error did not exceed 2 m. All computations are performed by the *M*-file orbits.

Often code observations are smoothed using the phase observations to achieve some reduction in the multipath error. The smoothing happens according to

$$\bar{\rho}(t_i) = \tfrac{1}{M}\rho(t_i) + \tfrac{M-1}{M}\Big(\bar{\rho}(t_{i-1}) + \lambda\big(\varphi(t_i) - \varphi(t_{i-1})\big)\Big)$$
$$\bar{\rho}(t_1) = \rho(t_1), \qquad M = 15.$$

We are not using any smoothing in our figures.

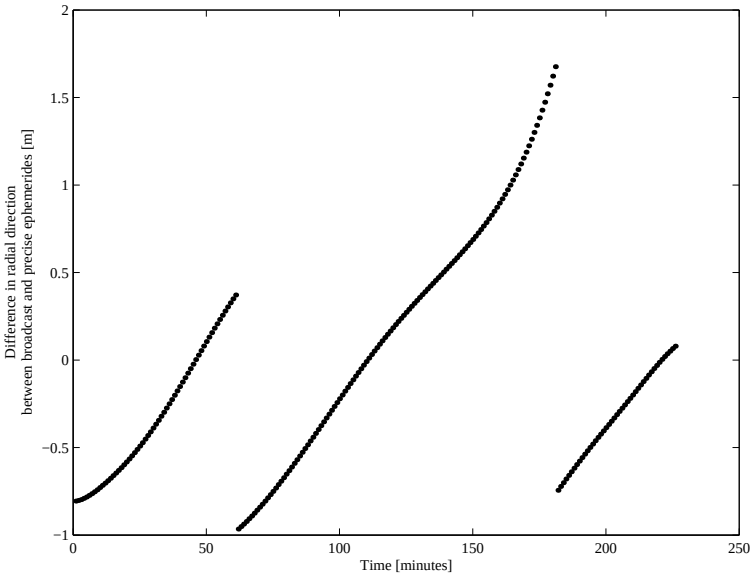

Figure 20.4 Lenght of difference vector between precise and broadcast ephemerides as projected onto the line of sight

References

Misra, Pratap, Burke, Brian P., & Pratt, Michael M. (1999). GPS performance in navigation. *Proceedings of the IEEE*, 87:65–85.